Metabolism Clinical and Experimental 127 (2022) 154936

Contents lists available at ScienceDirect

Metabolism Clinical and Experimental

journal homepage: www.metabolismjournal.com

Basic Science

Sodium/glucose cotransporter 2 (SGLT2) inhibitors improve cardiac function by reducing JunD expression in human diabetic hearts

Raffaele Marfella [a,b,*], Nunzia D'Onofrio [c], Maria Consiglia Trotta [d], Celestino Sardu [a], Lucia Scisciola [a], Cristiano Amarelli [e], Maria Luisa Balestrieri [d], Vincenzo Grimaldi [a], Gelsomina Mansueto [a], Salvatore Esposito [f], Michele D'Amico [d], Paolo Golino [g], Giuseppe Signoriello [h], Marisa De Feo [i], Ciro Maiello [e], Claudio Napoli [a,1], Giuseppe Paolisso [a,b,1]

[a] Department of Advanced Medical and Surgical Sciences, Università degli Studi della Campania "Luigi Vanvitelli", 80138 Naples, Italy
[b] Mediterranea Cardiocentro, Naples, Italy
[c] Department of Precision Medicine, the University of Campania "Luigi Vanvitelli", 80138 Naples, Italy
[d] Department of Experimental Medicine, University of Campania "Luigi Vanvitelli", 80138 Naples, Italy
[e] Unit of Cardiac Surgery and Transplants, AORN Ospedali dei Colli-Monaldi Hospital, 80131 Naples, Italy
[f] Unit of Pathological Anatomy, Aversa Hospital, Caserta, Italy
[g] Cardiology Division, University "L. Vanvitelli" - Monaldi Hospital, 80131 Naples, Italy
[h] Statistical Unit, Department of Mental Health and Public Medicine, University of Campania, Naples, Italy
[i] Department of Cardio-Thoracic Sciences, University of Campania "Luigi Vanvitelli", Naples, Italy

ARTICLE INFO

Article history:
Received 4 August 2021
Accepted 9 November 2021

Keywords:
Diabetic cardiomyopathy
JunD
SGLT2i

ABSTRACT

Background: The pathogenesis of experimental diabetic cardiomyopathy may involve the activator protein 1 (AP-1) member, JunD. Using non-diabetic heart transplant (HTX) in recipients with diabetes, we examined the effects of the diabetic milieu (hyperglycemia and insulin resistance) on cardiac JunD expression over 12 months. Because sodium/glucose cotransporter-2 inhibitors (SGLT2i) significantly reverse high glucose-induced AP-1 binding in the proximal tubular cell, we investigated JunD expression in a subgroup of type 2 diabetic recipients receiving SGLT2i treatment.

Methods: We evaluated 77 first HTX recipients (40 and 37 patients with and without diabetes, respectively). Among the recipients with diabetes, 17 (45.9%) were receiving SGLT2i treatment. HTX recipients underwent standard clinical evaluation (metabolic status, echocardiography, coronary computed tomography angiography, and endomyocardial biopsy). In the biopsy samples, we evaluated JunD, insulin receptor substrates 1 and 2 (IRS1 and IRS2), peroxisome proliferator-activated receptor-γ (PPAR-γ), and ceramide levels using real-time polymerase chain reaction and immunofluorescence. The biopsy evaluations in this study were performed at 1–4 weeks (basal), 5–12 weeks (intermediate), and up to 48 weeks (final, end of 12-month follow-up) after HTX.

Results: There was a significant early and progressive increase in the cardiac expression of JunD/PPAR-γ and ceramide levels, along with a significant decrease in IRS1 and IRS2 in recipients with diabetes but not in those without diabetes. These molecular changes were blunted in patients with diabetes receiving SGLT2i treatment.

Conclusion: Early pathogenesis in human diabetic cardiomyopathy is associated with JunD/PPAR-γ overexpression and lipid accumulation following HTX in recipients with diabetes. Remarkably, this phenomenon was reduced by concomitant therapy with SGLT2i, which acted directly on diabetic hearts.

1. Introduction

The pathogenesis of human diabetic cardiomyopathy is still under active investigation [1]. The specific hallmark of early cardiac damage characterizing diabetic cardiomyopathy occurs in the absence of coronary heart disease, valvular disease, hypertension, and/or dyslipidemia [2]. Moreover, insulin resistance and hyperglycemia are independent risk factors for the development of diabetic cardiomyopathy [3–5].

Abbreviations: ALCOA, Attributable, Legible, Contemporaneous, Original and Accurate; AP-1, activator protein 1; DSA, donor-specific antibodies; EMB, endomyocardial biopsy; HIF-1α, hypoxia-inducible factor-1α; HOMA-IR, homeostatic model assessment of insulin resistance; HTX, heart transplant; IRS-1, insulin receptor substrate 1; IRS-2, insulin receptor substrate 2; ISHLT, International Society for Heart Lung Transplantation; IVS, interventricular septum; PPAR-γ, peroxisome proliferator-activated receptor-γ; RT-PCR, real-time polymerase chain reaction; SGLT2i, sodium/glucose cotransporter 2 inhibitors.

* Corresponding author at: Piazza Miraglia, 2, 80138 Napoli, Italy.
E-mail address: raffaele.marfella@unicampania.it (R. Marfella).

[1] Equally shared senior authorship.

https://doi.org/10.1016/j.metabol.2021.154936

Recent experimental data have identified the activator protein 1 (AP-1) member, JunD, as a critical modulator of heart function in diabetic mice, and the main translational results were confirmed in heart samples from cardiac surgery patients [6,7]. Costantino et al. [6] showed that the transcription factor JunD participates in heart dysfunction through peroxisome proliferator-activated receptor-γ (PPAR-γ). Hussain et al. [7] reported hyperglycemia-induced JunD downregulation and myocardial dysfunction. Although these observations demonstrate a correlation between JunD expression and cardiac function, the data from cross-sectional human observations have not clarified the role of JunD in the function of the diabetic heart. Thus, to date, it is not yet known whether JunD may play a role in the initiation and progression of human diabetic cardiomyopathy and whether JunD modulation may reduce the influence of diabetes on heart function.

In this context, a study by Panchapakesan et al. first demonstrated that sodium/glucose cotransporter 2 inhibitors (SGLT2i) significantly reversed high glucose-induced AP-1 binding in proximal tubular cells [8]. SGLT2i are increasingly prescribed to treat patients with type 2 diabetes to reduce the risk of cardiovascular events, including heart failure. The mechanisms by which SGLT2i reduce this risk are likely to be independent of diabetes status and improvement of glycemic control [9,10]. Thus, the reduction of adverse cardiovascular outcomes suggests that SGLT2i may have plausible class effects on cardiorenal outcomes. Therefore, several theories of the mechanism of action of SGLT2i in heart failure have been postulated [11,12]. First, SGLT-2i could affect cardiovascular risk factors, such as improving the metabolic profile; reducing plasma glucose levels, blood pressure, and body weight; and modifying the lipid profile. Second, SGLT2i induce a diuretic effect by reducing the interstitial volume much more than reducing the intravascular volume, which is a key factor in preventing fluid overload and exacerbation of heart failure that requires hospitalization. Finally, SGLT2i could produce a hemodynamic response that creates a favorable environment to reduce cardiac hydrostatic pressure to induce ventricular remodeling and hypertrophy. However, there are no data on the effects of SGLT2i on the metabolic molecular mechanisms in human heart cardiomyocytes affected by the diabetic milieu. Therefore, to gain relevant insights into the metabolic mechanisms influenced by diabetic status, we studied JunD expression at the onset of human diabetic cardiomyopathy by evaluating biopsy samples of transplanted hearts following our previous model [13]. We also investigated cardiac JunD expression in a subgroup of recipients with type 2 diabetes receiving SGLT2i treatment.

2. Methods

2.1. Patients

From January 2010, we conducted a prospective ongoing study (diabetic cardiomyopathy-AHEAD study, NCT03546062) [13] under the ALCOA (Attributable, Legible, Contemporaneous, Original and Accurate) integrity protocols with a 12-month follow-up of patients who underwent first heart transplant (HTX) at the HTX referral center of Monaldi Hospital, Region Campania according to International Society for Heart and Lung Transplantation (ISHLT) guidelines [14]. The study was approved by the ethics committee (prot. 438), and the patients provided written informed consent. We selected 77 consecutive patients who underwent HTX from January 2016 and were followed-up for 12 months among the AHEAD study population. The study population was divided into two groups according to the presence or absence of pre-transplantation type 2 diabetes. Patients with type 2 diabetes for at least 6 months before HTX, with optimal glycemic control (HbA1c <7%) and without diabetic complications, were included according to the ISHLT guidelines [14]. Among patients with diabetes, patients who never used SGLT2i were classified as "non-SGLT2i-treated patients with diabetes." Patients with type 2 diabetes who had already used SGLT2i (empagliflozin, dapagliflozin, canagliflozin) for at least 6 months before the HTX and continued throughout the follow-up were classified as "SGLT2i-treated patients with diabetes." Patients with endomyocardial biopsy specimens consistent with ISHLT grade 2R considered positive for rejection, positive donor-specific antibodies (DSA), increased T4/T8 ratio, positive IgM and/or IgG cytomegalovirus antibodies, and post-HTX diabetes were excluded from the study. The surgical technique used has been previously described in detail [13]. All patients underwent immunosuppression therapy consisting of induction with polyclonal anti-lymphocyte antibodies and maintenance therapy mainly based on cyclosporine or tacrolimus, mycophenolate mofetil, mycophenolate mofetil, everolimus, and prednisone [13].

2.2. Clinical and echocardiographic evaluations

The internationally accepted evaluations (clinical and instrumental evaluation and glycemic control, i.e., fasting glycaemia and HbA1c) were performed at weeks 1, 24, and 48 after HTX [14]. Homeostatic model assessment for insulin resistance (HOMA-IR) and systemic insulin resistance was evaluated before HTX (before starting immunosuppressive therapy) and at week 48 after HTX during immunosuppressive therapy. We performed echocardiographic evaluations of systolic (ejection fraction [EF] and tricuspid annular plane systolic excursion [TAPSE]) and diastolic (E/e′ ratio) heart function at baseline and after a 12-month follow-up, as previously described [15,16].

2.3. Heart biopsies

After HTX, endomyocardial biopsies from all patients were obtained either as routine surveillance protocols or diagnostic tools for allograft dysfunction and clinically suspected rejection [13,14]. The standard biopsy schedule was performed weekly for the first month, every 2 weeks for the next month, once for the next 4 weeks, once for the next 6 weeks, then every 3 months for the next two years, and every 6 months subsequently as indicated by the guidelines for HTX [14]. In our study, we evaluated the biopsies performed 1 year after HTX. Biopsies were performed as described previously [13]. Endomyocardial biopsy specimens, without histological rejection signs, were analyzed for cellular viability by evaluating hypoxia-inducible factor-1α (HIF-1α). Although the study was based on prospective biopsies of implanted hearts, an experienced thoracic surgeon excised 4–6 tissue specimens approximately 5–10 mm^3 in size from the left ventricular free wall. Tissues were immediately treated and analyzed as described previously [13].

2.4. Tissue analysis

The biopsy evaluations in the study were performed: 1–4 weeks (basal), 5–12 weeks (intermediate), and up to 48 weeks (final, end of 12-month follow-up) after HTX. Two biopsy specimens for each patient at each period (basal, intermediate, and final) were embedded in Tissue-Tek OCT in aluminum molds, frozen quickly in liquid nitrogen, and stored at −80 °C until real-time polymerase chain reaction (RT-PCR). The other two-biopsy specimens for each patient from each period (basal, intermediate, and final) were immediately immersion-fixed in 10% buffered formalin. In all study populations, the specimens of each period (basal, intermediate, and final) were analyzed up to 30 days after the end of follow-up.

The RT-PCR RNeasy Mini kit (74106, Qiagen) was used to perform total RNA isolation from human heart sample homogenates according to the manufacturer's protocols for "Stabilization of RNA in Harvested Animal Tissues" and "Purification of Total RNA from Animal Tissues." A NanoDrop 2000c Spectrophotometer (Thermo Fisher Scientific) was used to evaluate RNA concentration and purity. After the elimination of genomic DNA (gDNA) contamination from heart samples, mRNA was reverse transcribed to cDNA (reverse transcription step) using the Gene AMP PCR System 9700 (Applied Biosystems) and QuantiTect

Reverse Transcription kit (205311, Qiagen) following the manufacturer's protocol for "Reverse Transcription with Elimination of Genomic DNA for Quantitative, Real-Time PCR." cDNA amplification (RT-PCR step) was performed using a CFX96 Real-time System C1000 Touch Thermal Cycler (Bio-Rad), according to the protocol "Two-Step RT-PCR (Standard Protocol)." The QuantiTect SYBR Green PCR Kit (204,143, Qiagen) was used along with specific QuantiTect Primer Assays to detect human JunD (QT00200067, Qiagen), insulin receptor substrate 1 (IRS1) (QT00074144, Qiagen), insulin receptor substrate 2 (IRS2) (QT00064036, Qiagen), peroxisome proliferator-activated receptor-gamma (PPARγ) (QT00029841, Qiagen), β-actin (ACTB) (QT00095431, Qiagen), and GAPDH (QT00079247, Qiagen). P-values were calculated based on a Student's *t*-test or one-way analysis of variance (ANOVA), followed by Tukey's multiple comparisons tests; $P < 0.05$ was considered significant.

2.4.1. Immunofluorescence analysis

We used confocal laser-scanning microscopy to evaluate JunD, IRS1, IRS2, PPAR-γ, and ceramide myocardial localization. Immunofluorescence analysis of myocardial sections was performed following the manufacturer's protocol using a confocal laser-scanning microscope (LSM 700; Zeiss). Immunofluorescence analysis was performed in deparaffinized basal, intermediate, and final heart sections from patients without diabetes and SGLT2i-treated and non-SGLT2i-treated patients with diabetes. Briefly, deparaffinized sections were subjected to antigen retrieval buffer (10 mM sodium citrate, 0.05% Tween 20, pH 6.0) and heated in a microwave for 20 min. Slides were then washed twice in phosphate-buffered saline (PBS) and incubated for 30 min in Tris-buffered saline (TBS) containing 50 mM ammonium chloride to reduce background fluorescence. Permeabilization was performed by incubation with 0.2% Triton X-100 in PBS for 5 min at room temperature. All sections were blocked for 1 h at room temperature with fetal bovine serum (FBS) and saponin (0.1 g/ml) and stained with the following primary antibodies: anti-JunD antibody [EPR17365] (1:300, ab181615, Abcam), anti-IRS1 antibody (1:500, ab131487, Abcam), anti-IRS2 antibody [EPR904(2)] (1:500, ab134101, Abcam), anti-PPAR gamma antibody (1:500, ab45036, Abcam), anti-ceramide (1:100, MID 15B4, Enzo ALX-804-196-T050). All slides were co-immunolabeled with antibodies against cardiac troponin T [1C11] (1:500, ab87436, Abcam) for 16 h. After incubation for 1 h at room temperature with secondary antibodies labeled with Alexa Fluor 488 or 633 diluted at 1:1000 in blocking solution, sections were quenched for autofluorescence using the Vector TrueVIEW Autofluorescence Quenching Kit (VEC-SP-8500, Vector Laboratories, catalog no.VEC-SP-8500-15). The true staining and absence of autofluorescence and non-specific staining caused by non-specific interactions of immunoglobulin molecules with the tissue was ensured by incubating myocardial sections with blocking solution, supplemented with a non-immune immunoglobulin IgG or IgM antibody, followed by incubation with secondary antibody labeled with Alexa Fluor 488 and Alexa Fluor 633 for 1 h at room temperature. All samples were stained with 4,6-diamidino-2-phenylindole (DAPI, 5 μg/ml) for 10 min before mounting in Vectashield Mounting Medium (Vector Laboratories, catalog no. H-1700). Using a Zeiss LSM 710 confocal microscope, slides were imaged using a plan apochromat ×63 (NA 1.4) oil immersion objective [17,18]. The non-specific fluorescence signal obtained from the negative control was subtracted as the background. Representative confocal laser-scanning microscopy images of immunofluorescence assay negative controls from patients without diabetes, and non-SGLT2i-treated and SGLT2i-treated patients with diabetes at 1–4 weeks (basal), 5–12 weeks (intermediate), and up to 48 weeks (final, end of 12-month follow-up) after HTX, supplemented with (A) a non-immune immunoglobulin IgG antibody or (B) a non-immune immunoglobulin IgM antibody followed by incubation with secondary antibody labeled with Alexa Fluor 488 and Alexa Fluor 633 for 1 h at room temperature is reported in the supplementary figure. All samples were stained with DAPI (5 μg/ml) for 10 min before mounting in Vectashield Mounting Medium (Vector Laboratories, Burlingame, CA, USA). All slides were imaged using a Zeiss LSM 710 confocal microscope (Zeiss, Oberkochen, Germany) with a plan apochromat ×63 (NA1.4) oil immersion objective.

2.4.2. IRS1 and PPARϒ phosphorylated in heart tissue

Phospho IRS1 (P-IRS1) and phospho PPAR gamma (P-PPARγ) levels were analyzed in cardiac tissue protein homogenates using enzyme-linked immunosorbent assay (ELISA). P-IRS1 was analyzed using a commercial ELISA kit (KHO0521 IRS1 (Phospho) [pS312] Human ELISA Kit, Invitrogen), while a specific human anti-P-PPARγ, suitable for ELISA assays, was used according to the manufacturer's ELISA protocol (Anti-PPAR Gamma Phospho-ser273 antibody orb158188 – biorbyt).

2.4.3. Triacylglycerol and ceramide measurements in heart tissue

A solution (500 μl) of 2 mM NaCl/20 mM EDTA/50 mM sodium phosphate buffer (pH 7.4) was added to the myectomy samples removed from the LV septum. Then, 10 μl of the homogenate was mixed with 10 μl of tert-butyl alcohol and 5 μl of Triton X-100/methyl alcohol mixture (1:1 v/v) for lipid extraction. Triacylglycerol was measured using a Triglyceride Assay Kit (Abcam-Quantification ab65336). Ceramide content was measured using a Human Ceramide ELISA Kit (Biosource, MBS7254089).

2.5. Statistical analysis

Data are expressed as mean ± SD for continuous variables and percentages for categorical variables. We used linear mixed models to analyze any difference in the levels of JunD IRS1, IRS2, and PPARγ between groups over the first and second period after verifying the assumption of sphericity using the Mauchly test. Interaction effects were assessed to determine within-group changes and between-group differences between the first and second time points. Bonferroni correction was used to compare post-hoc main effects.

The Shapiro–Wilk test was used to evaluate the normality of the data. Statistical significance was set at $P < 0.05$. Data were analyzed using SPSS software (version 23). A sample size of 77 patients was required to detect an effect size of 0.20 for within-group changes using repeated measures analysis of variance (ANOVA) with a power of 0.80, and three measurements per group, assuming a correlation between repeated measures of 0.40 (G-Power 3.1.9.4).

3. Results

3.1. Baseline characteristics and outcomes at 1-year follow-up

The characteristics of HTX recipients and donors are listed in Table 1. We report data from 40 patients without diabetes (51.9%), 20 patients with type 2 diabetes not treated with SGLT2i (25.9%), and 17 patients with type 2 diabetes treated with SGLT2i (22.2%). Among SGLT2i-treated patients with type 2 diabetes, 10 were treated with empagliflozin, five with dapagliflozin, and two with canagliflozin throughout the observation period. The study groups were well matched, as indicated by the guideline criteria for entry into the transplantation program (Table 1). Compared with patients without pretransplant diabetes, patients who had pretransplant diabetes spent significantly more time in the hospital during the first year after HTX. The mean duration of hospitalization was 22 days (median, 16 days; maximum, 73 days) for recipients who had pretransplant diabetes and 17 days for recipients who did not (median, 13 days; maximum, 68 days). None of the other baseline characteristics differed significantly between groups, including preoperative creatinine and cholesterol levels. Anti-diabetic therapy in patients with pretransplant diabetes is reported in Table 1. Diabetes duration was 15.1 ± 3.3 years in the non-SGLT2i-treated patients with diabetes and 16.1 ± 1.9 years in the SGLT2i-treated patients with diabetes ($P = 0.275$). None of the patients with diabetes in the study had diabetic complications, such as nephropathy, neuropathy, or retinopathy.

Table 1
Baseline and follow-up clinical characteristics of the study population.

	Non-diabetic patients			No-SGLT2i diabetic patients			SGLT2i diabetic patients		
	Basal	Follow-up	P	Basal	Follow-up	P	Basal	Follow-up	P
N	40	40	/	20	20	/	17	17	/
Mean age (years)	50.9 ± 6.0	/	/	52.7 ± 5.5	/	/	51.3 ± 6.0	/	/
Sex, male (%)	29 (72)	/	/	17 (85)	/	/	13 (76)	/	/
BMI (kg/m^2)	25.1 ± 1.1	24.6 ± 0.87	0.024	26.6 ± 1.66*	25.7 ± 1.65*	0.107	26.4 ± 1.74*	26.2 ± 1.60*	0.684
Etiology of heart failure, n (%)									
Ischemic cardiomyopathy	16 (40)	/	/	9 (45)	/	/	8 (47)	/	/
Dilated cardiomyopathy	14 (35)	/	/	6 (30)	/	/	6 (35)	/	/
Other	10 (25)	/	/	5 (25)	/	/	3 (18)	/	/
Cardiovascular risk factors, n (%)									
Hypertension, n (%)	7 (17)	/	/	3 (15)	/	/	2 (12)	/	/
Dyslipidemia, n (%)	13 (32)	/	/	8 (40)	/	/	8 (47)	/	/
Family history of CAD, n (%)	13 (32)	/	/	8 (40)	/	/	7 (41)	/	/
Laboratory analyses									
Plasma glucose (mg/dl)	90.5 ± 5.1	93.4 ± 6.5	0.027	113.4 ± 27.8*	111.6 ± 13.7*	0.656	117.3 ± 14.9*	116.5 ± 8.5*	0.773
HbA1c (%)	4.9 ± 0.37	5.0 ± 0.61	0.934	6.61 ± 1.08*	5.68 ± 0.81*	0.001	6.54 ± 0.67*	5.91 ± 0.98*	0.011
HOMA-IR	1.45 ± 0.31	1.48 ± 0.18	0.173	4.46 ± 0.59*	5.61 ± 0.49*	0.002	4.47 ± 0.37*	4.81 ± 0.66*,§	0.038
Cholesterol (mg/dl)	155.6 ± 20.2	151.5 ± 17.7	0.364	178.4 ± 19.5*	162.5 ± 16.5	0.003	176.1 ± 18.3	159.7 ± 33.7	0.025
LDL-cholesterol (mg/dl)	92.1 ± 19.5	89.3 ± 18.0	0.522	100.1 ± 16.5*	90.9 ± 12.4	0.011	97.7 ± 13.7*	88.4 ± 13.2	0.524
HDL-cholesterol (mg/dl)	41.0 ± 1.27	40.1 ± 2.29	0.052	40.8 ± 2.29	40.5 ± 2.30	0.643	40.1 ± 4.10	40.6 ± 2.03	0.161
Triglycerides (mg/dl)	112.2 ± 7.16	110.2 ± 11.1	0.330	181.5 ± 35.2*	148.9 ± 30.1*	0.001	190.9 ± 27.8*	162.1 ± 20.3*	0.004
Creatinine (mg/dl)	1.0 ± 0.26	1.0 ± 0.11	0.212	1.1 ± 0.16	1.1 ± 0.21	0.122	1.1 ± 0.24	1.1 ± 0.82	0.168
Anti-diabetic therapy									
Insulin, n (%)	/	/	/	4 (20)	/	/	3 (18)	/	/
DPP-IV inhibitor, n (%)	/	/	/	7 (35)	/	/	5 (29)	/	/
GLP-1 agonist, n (%)	/	/	/	3 (15)	/	/	2 (12)	/	/
Sulfonylureas, n (%)	/	/	/	3 (15)	/	/	2 (12)	/	/
Glinides, n (%)	/	/	/	4 (20)	/	/	3 (18)	/	/
Metformin, n (%)	/	/	/	12 (60)	/	/	11 (65)	/	/
Donor data									
Mean age (years)	31.2 ± 11.8	/	/	30.7 ± 12.2	/	/	31.1 ± 11.9	/	/
Sex, male (%)	22 (55.0)	/	/	12 (60.0)	/	/	10 (58.8)	/	/
BMI (kg/m^2)	26.2 ± 1.1	/	/	26.3 ± 1.3	/	/	26.4 ± 1.0	/	/
Donor ischemic time (min)	100.7 ± 22.2	/	/	101.5 ± 20.9	/	/	102.7 ± 22.8	/	/

HOMA-IR = homeostatic model assessment for insulin resistance. DPP-IV = dipeptidyl peptidase IV; GLP-1 = glucagon-like peptide-1. Data are means ± SD or n (%).
* $P < 0.01$ vs. non-diabetic patients.
§ $P < 0.01$ vs. no-SGLT2i.

Before HTX and during the follow-up, patients with diabetes showed optimal glucose (HbA1c ≤ 7%) and lipid control (Table 1). As expected, plasma glucose levels and systemic insulin resistance (HOMA-IR) were higher in patients with diabetes than in patients without diabetes at baseline and follow-up (Table 1).

Among patients with diabetes, the plasma glucose levels were similar in those who did and did not receive SGLT2i treatment at baseline and follow-up (Table 1). Interestingly, systemic insulin resistance (HOMA-IR) increased in all patients at follow-up, probably due to immunosuppressive therapy. However, the HOMA-IR increase was significantly higher in non-SGLT2i-treated patients with diabetes than in SGLT2i-treated patients with diabetes at follow-up (Table 1). After HTX, the in-hospital echocardiographic evaluation showed a normal ejection fraction, slight alterations in the diastolic phase, and right ventricular function throughout the studied population, without significant differences between patients with and without diabetes (Fig. 1). After 12 months of follow-up, both left and right ventricular function with a significant reduction in ejection fraction and TAPSE were significantly lower in patients with diabetes than in those without diabetes ($P < 0.05$) (Fig. 1). Finally, the E/e′ ratio showed a lower reduction among patients with diabetes (Fig. 1).

Interestingly, the impairment of cardiac function was smaller in patients with diabetes treated with SGLT2i. In fact, the worsening of cardiac function was less evident in the SGLT2i-treated patients with diabetes. As shown in Fig. 1, the E/e′ ratio was significantly lower and the ejection fraction was significantly higher in SGLT2i-treated patients than in patients with diabetes treated without SGLT2i. Among patients with type 2 diabetes treated with SGLT2i, there was no difference between the different SGLT2i treatments (data not shown).

3.2. Molecular analysis of ventricular specimens

As evidenced by colocalization immunofluorescence images of myocardial sections, JunD, PPAR-γ, IRS1, IRS2, and ceramide were localized in the cardiomyocytes of patients with (irrespective of SGLT2i treatment status) and without diabetes (Figs. 2–5). Interestingly, PCR analysis showed that JunD, PPAR-γ, IRS1, and IRS2 levels, as well as phosphorylated IRS1 and PPAR-γ levels, were similar in heart endomyocardial biopsies from all groups during the basal period (Supplementary Fig. 2). During the intermediate period, JunD and PPAR-γ levels were higher, and IRS1 and IRS2 levels were lower in specimens from patients with diabetes treated without SGLT2i than in those treated with SGLT2i or patients without diabetes. These variations were also observed in phosphorylated IRS1 and PPAR-γ levels (Supplementary Fig. 2). At the 12-month follow-up, these differences became more pronounced, reaching statistical significance (Figs. 2–5). Among patients with type 2 diabetes treated with SGLT2i, there was no difference between the different SGLT2i treatments (data not shown). The differences in myocardial JunD, PPAR-γ, IRS1, and IRS2 levels observed among the diabetic groups were independent of glycemic control, as shown by the plasma glucose values during follow-up (Table 1). Scatter plots show how the values of EF, E/e′, and TAPSE varied with the levels of JunD in the heart (Fig. 6).

3.3. Lipid accumulation in cardiomyocytes

As shown in Fig. 7, the triacylglycerol and ceramide measurements in heart tissue (cardiomyocytes) revealed similar lipid content in patients with and without diabetes. Interestingly, during the intermediate

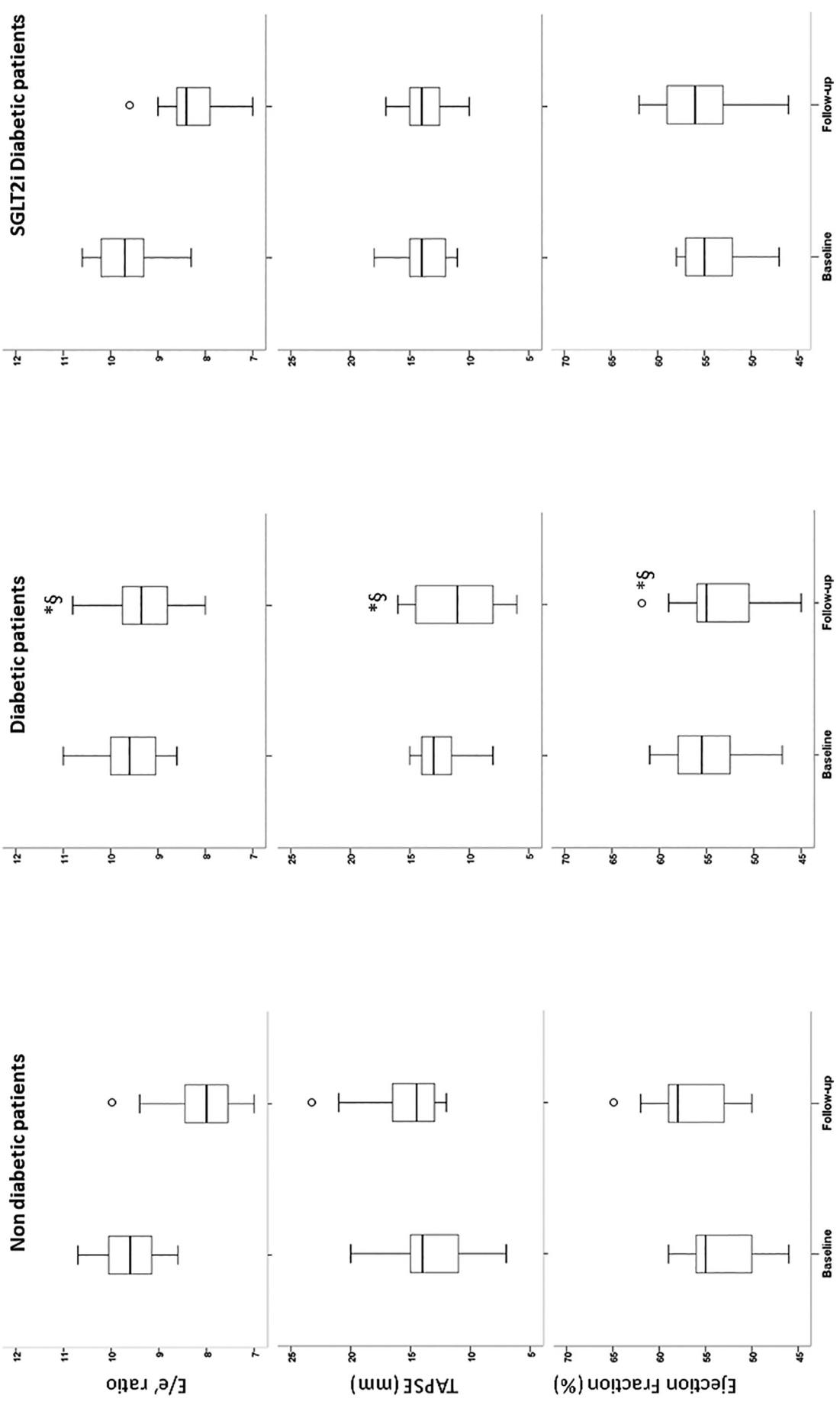

Fig. 1. Echocardiographic data from heart transplant patients at baseline and during follow-up. The ratio of transmitral Doppler early filling velocity to tissue Doppler early diastolic mitral annular velocity (E/e'), tricuspid annular plane systolic excursion (TAPSE), and cardiac ejection fraction at week 1 (Basal) and week 48 (Follow-up) after HTX, in patients without diabetes, non-sodium-glucose transport protein 2 inhibitors (SGLT2i)-treated patients with diabetes, and SGLT2i-treated patients with diabetes. Boxplot showing the median, 25th and 75th percentiles, and range. *P < 0.05 vs. patients without diabetes, §P < 0.05 vs. SGLT2i-treated patients with diabetes, °P < 0.05 vs. basal values.

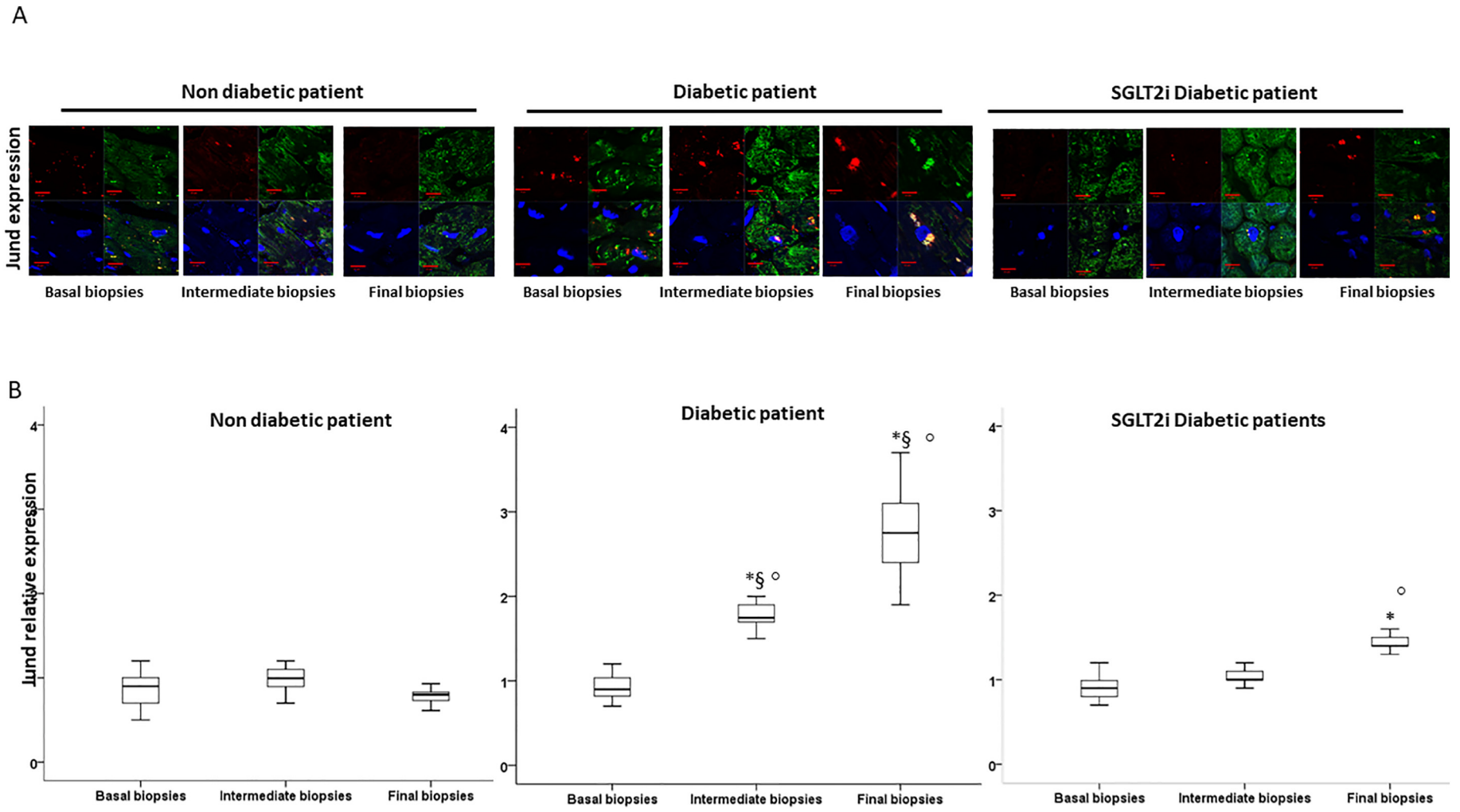

Fig. 2. JunD in myocardial biopsies at basal, intermediate, and final evaluations. Panel A, Representative confocal laser-scanning microscope images of JunD expression levels (red) in deparaffinized sections from patients without diabetes, non-SGLT2i-treated patients with diabetes, and SGLT2i-treated patients with diabetes at 1–4 weeks (Basal), 5–12 weeks (Intermediate) and up to 48 weeks (Final, End of 12-month follow-up) after HTX. Cardiac troponin T (green) was used to localize the immunofluorescence signal in cardiomyocytes, while 4′,6-diamidino-2-phenylindole (DAPI; 5 μg/ml) staining was used for nucleus counterstaining (blue). Upper left, JunD; upper right, troponin T; lower left, DAPI; lower right, merged. Scale bar = 10 μm. Panel B, JunD semiquantitative evaluation using RT-PCR in heart specimens from biopsies of patients without diabetes, non-SGLT2i-treated patients with diabetes, and SGLT2i-treated patients with diabetes at 1–4 weeks (Basal), 5–12 weeks (Intermediate) and up to 48 weeks (Final, end of 12-month follow-up) after HTX. Boxplot showing the median, 25th and 75th percentiles, and range. *P < 0.05 vs. patients without diabetes, §P < 0.05 vs. SGLT2i-treated patients with diabetes, °P < 0.05 vs. basal values.

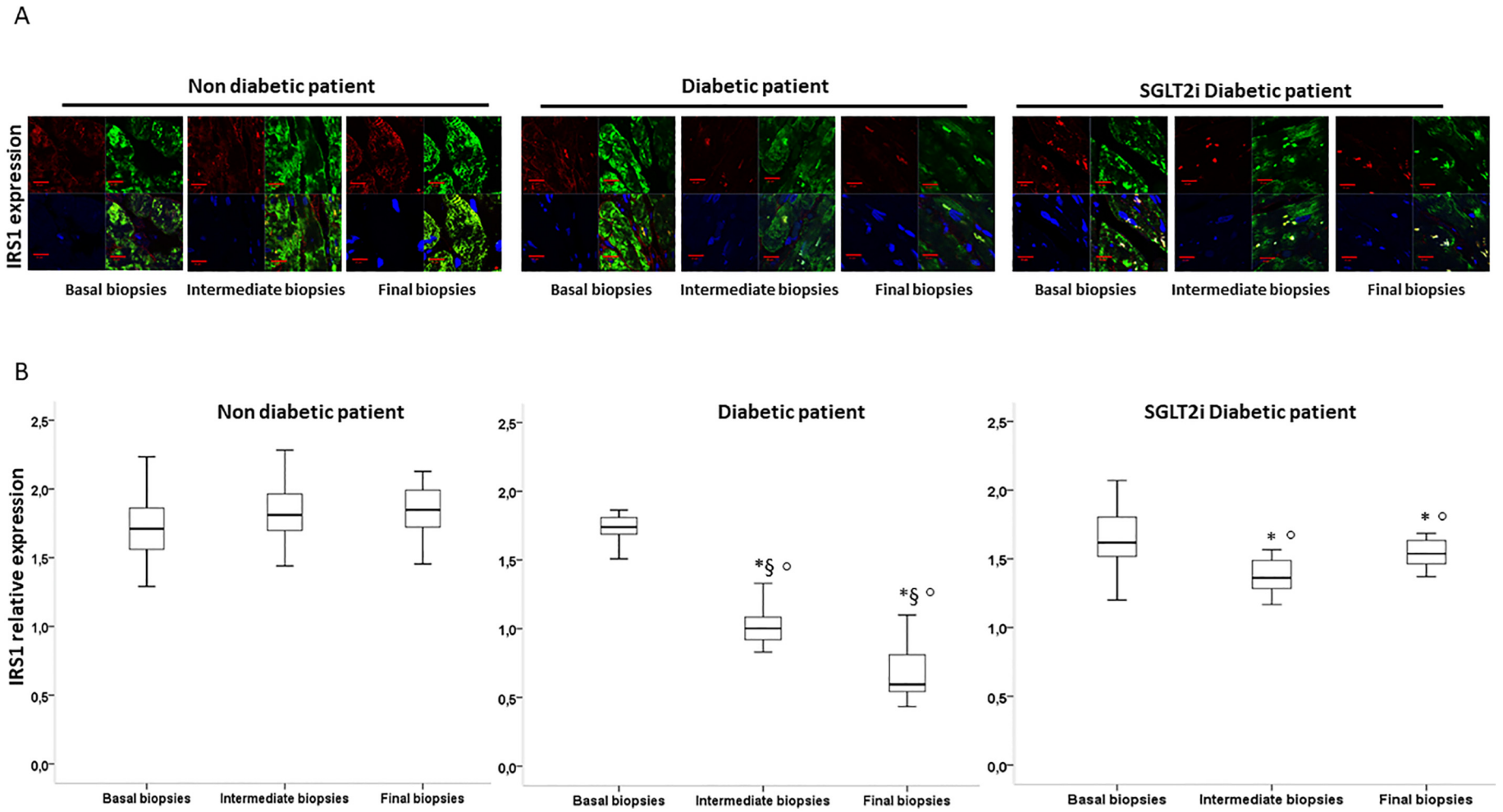

Fig. 3. Insulin receptor substrate 1 in myocardial biopsies at basal, intermediate, and final evaluations. Panel A, Indicative images of IRS1 RNA expression levels (red) obtained using the confocal laser-scanning microscopy of deparaffinized sections patients without diabetes, non-SGLT2i-treated patients with diabetes, and SGLT2i-treated patients with diabetes at 1–4 weeks (Basal), 5–12 weeks (Intermediate), and up to 48 weeks (Final, end of 12-month follow-up) after HTX. IRS1 localization in cardiomyocytes was ensured by using cardiac troponin T (green) co-immunofluorescence. 4′,6-Diamidino-2-phenylindole (DAPI; 5 μg/ml) was used for nuclei counterstaining (blue). Upper left, IRS1; upper right, troponin T; lower left, DAPI; lower right, merged. Scale bar = 10 μm. Panel B, IRS-1 semiquantitative evaluation using RT-PCR on heart specimens from biopsies of patients without diabetes, non-SGLT2i-treated patients with diabetes, and SGLT2i-treated patients with diabetes at 1–4 weeks (Basal), 5–12 weeks (Intermediate), and up to 48 weeks (Final, end of 12-month follow-up) after HTX. Boxplot showing the median, 25th and 75th percentiles, and range. *$P < 0.05$ vs. patients without diabetes, $^{§}P < 0.05$ vs. SGLT2i-treated patients with diabetes, °$P < 0.05$ vs. basal values.

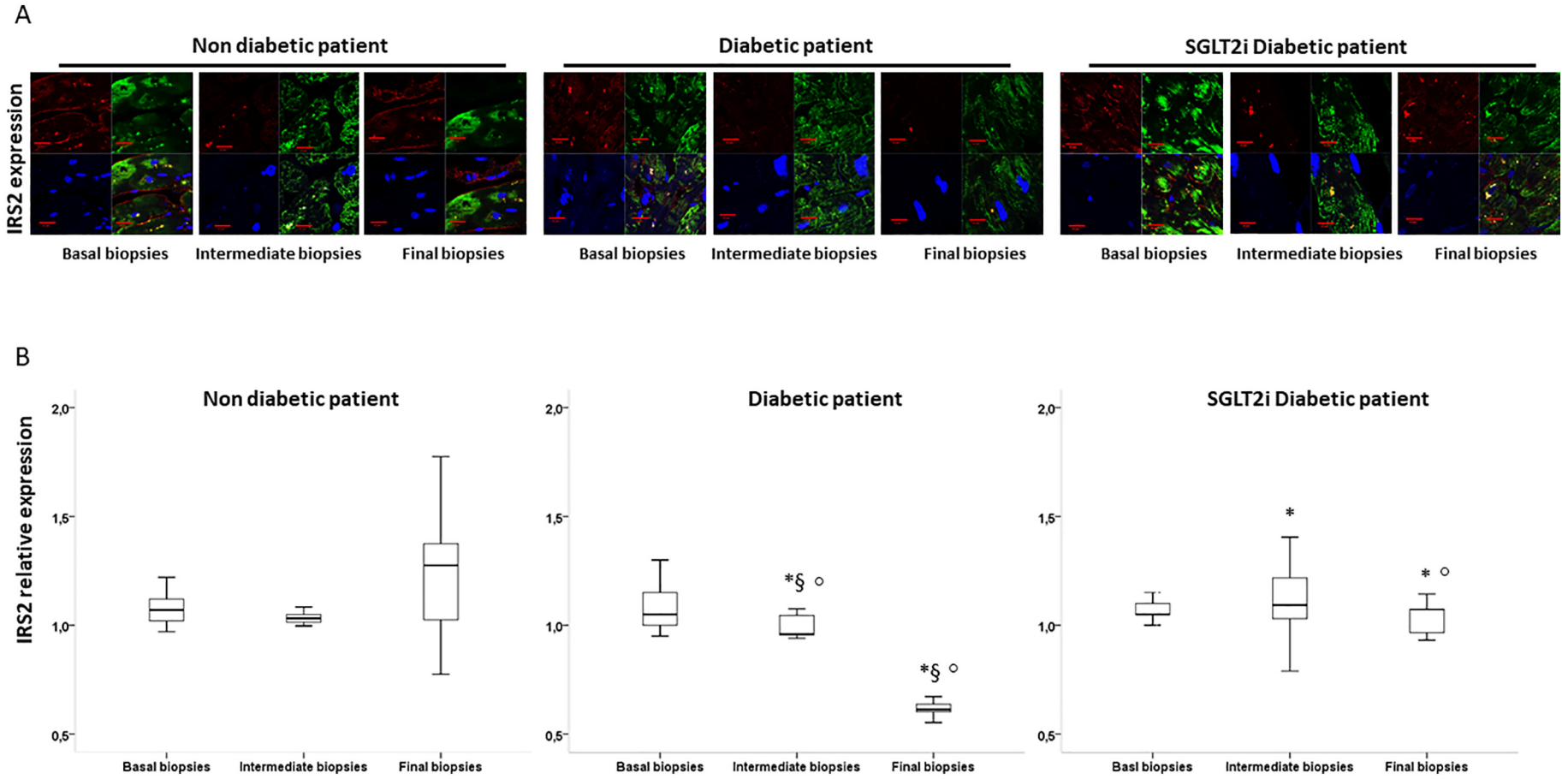

Fig. 4. Insulin receptor substrate 2 in myocardial biopsies at basal, intermediate, and final evaluations. Panel A, Illustrative images from confocal laser-scanning microscope analysis of IRS2 protein expression levels (red) in deparaffinized heart sections from patients without diabetes, non-SGLT2i-treated patients with diabetes, and SGLT2i-treated patients with diabetes at 1–4 weeks (Basal), 5–12 weeks (Intermediate), and up to 48 weeks (Final, end of 12-month follow-up) after HTX. IRS1 antibody was followed by cardiac troponin T (green) immunofluorescence staining. 4′,6-Diamidino-2-phenylindole (DAPI; 5 μg/ml) was used for nuclei counterstaining (blue). Upper left, IRS2; upper right, troponin T; lower left, DAPI; lower right: merged. Scale bar = 10 μm. Panel B, IRS-2 semiquantitative evaluation using RT-PCR in heart specimens from biopsies of patients without diabetes, non-SGLT2i-treated patients with diabetes, and SGLT2i-treated patients with diabetes at 1–4 weeks (Basal), 5–12 weeks (Intermediate), and up to 48 weeks (Final, end of 12-month follow-up) after HTX. Boxplot showing the median, 25th and 75th percentiles, and range. $^{*}P < 0.05$ vs. patients without diabetes, $^{§}P < 0.05$ vs. SGLT2i-treated patients with diabetes, $^{\circ}P < 0.05$ vs. basal values.

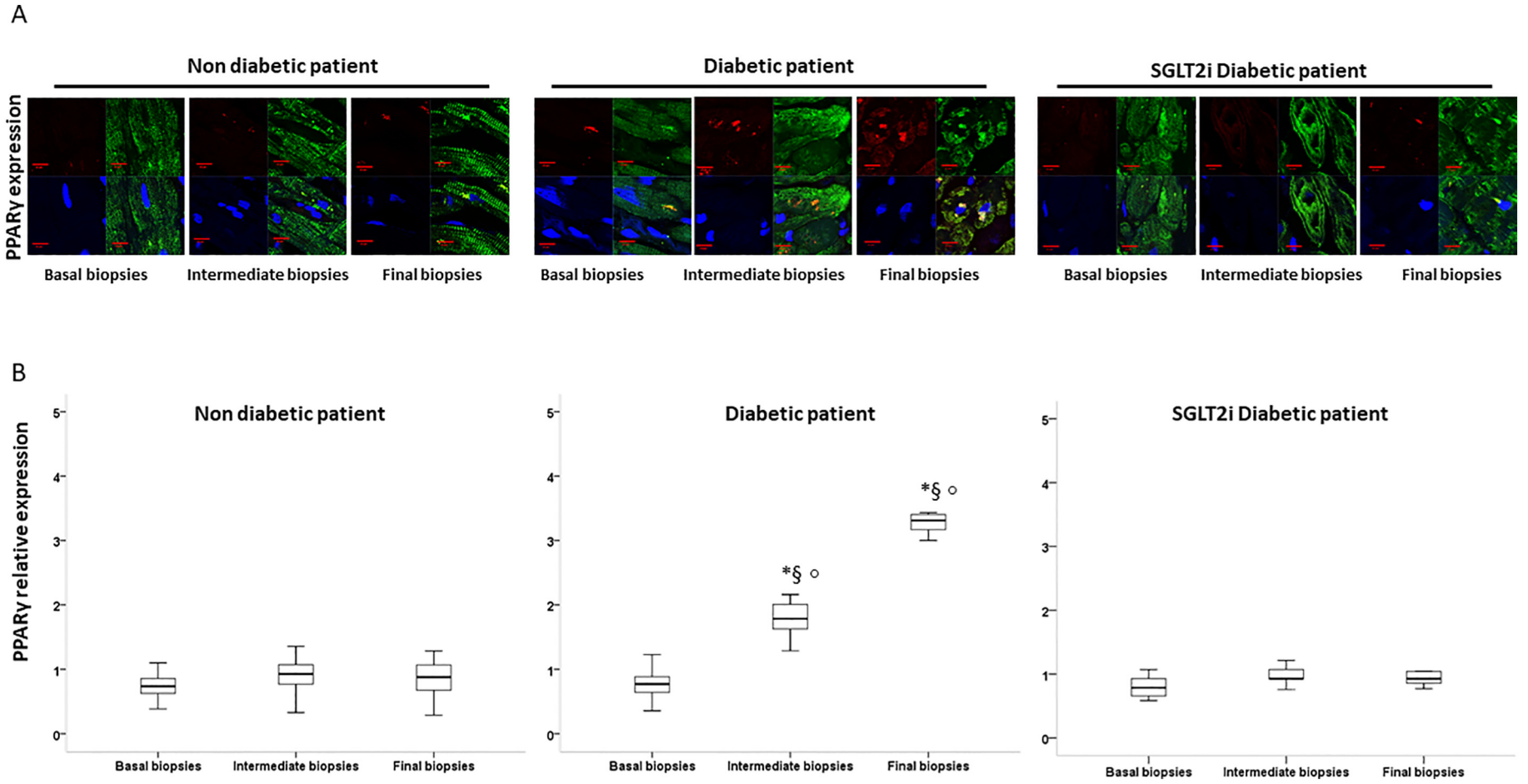

Fig. 5. Peroxisome proliferator-activated receptor-γ in myocardial biopsies at basal, intermediate, and final evaluations. Panel A, Representative confocal laser-scanning microscope images of PPARγ (red) expression levels in deparaffinized heart sections from patients without diabetes, non-SGLT2i-treated patients with diabetes, and SGLT2i-treated patients with diabetes at 1–4 weeks (Basal), 5–12 weeks (Intermediate), and up to 48 weeks (Final, end of 12-month follow-up) after HTX. Cardiac troponin T (green) immunofluorescence staining was used to localize PPARγ in cardiomyocytes. DAPI (blue) was used for nuclei counterstaining. Upper left, PPARγ; upper right, troponin T; lower left, DAPI; lower right, merged. Scale bar = 10 μm. Panel B, PPAR-γ semiquantitative evaluation using RT-PCR in heart specimens from biopsies patients without diabetes, non-SGLT2i-treated patients with diabetes, and SGLT2i-treated patients with diabetes at 1–4 weeks (Basal), 5–12 weeks (Intermediate), and up to 48 weeks (Final, end of 12-month follow-up) after HTX. Boxplot showing the median, 25th and 75th percentiles, and range. *$P < 0.05$ vs. patients without diabetes, §$P < 0.05$ vs. SGLT2i-treated patients with diabetes, °$P < 0.05$ vs. basal values.

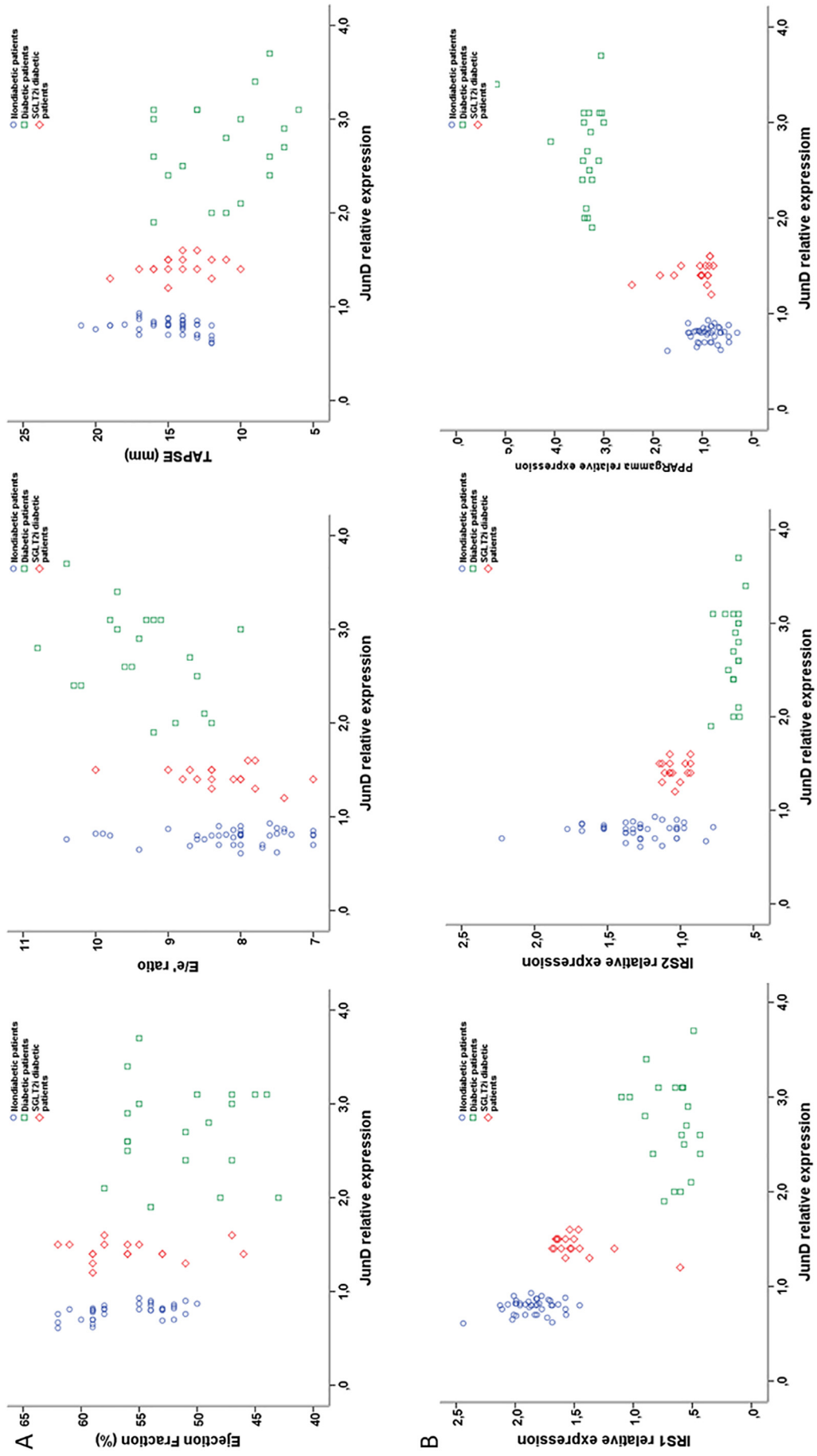

Fig. 6. Panel A, Scatter graph of mRNA JunD expression, the ratio of transmitral Doppler early filling velocity to tissue Doppler early diastolic mitral annular velocity (E/e'), tricuspid annular plane systolic excursion (TAPSE), and cardiac ejection fraction in the whole study population. Panel B, Scatter graph of myocyte JunD expression and insulin receptor substrate 1 (IRS-1), Insulin receptor substrate 2 (IRS-2), peroxisome proliferator-activated receptor gamma (PPAR-γ), and ceramide myocardial levels in the whole study population.

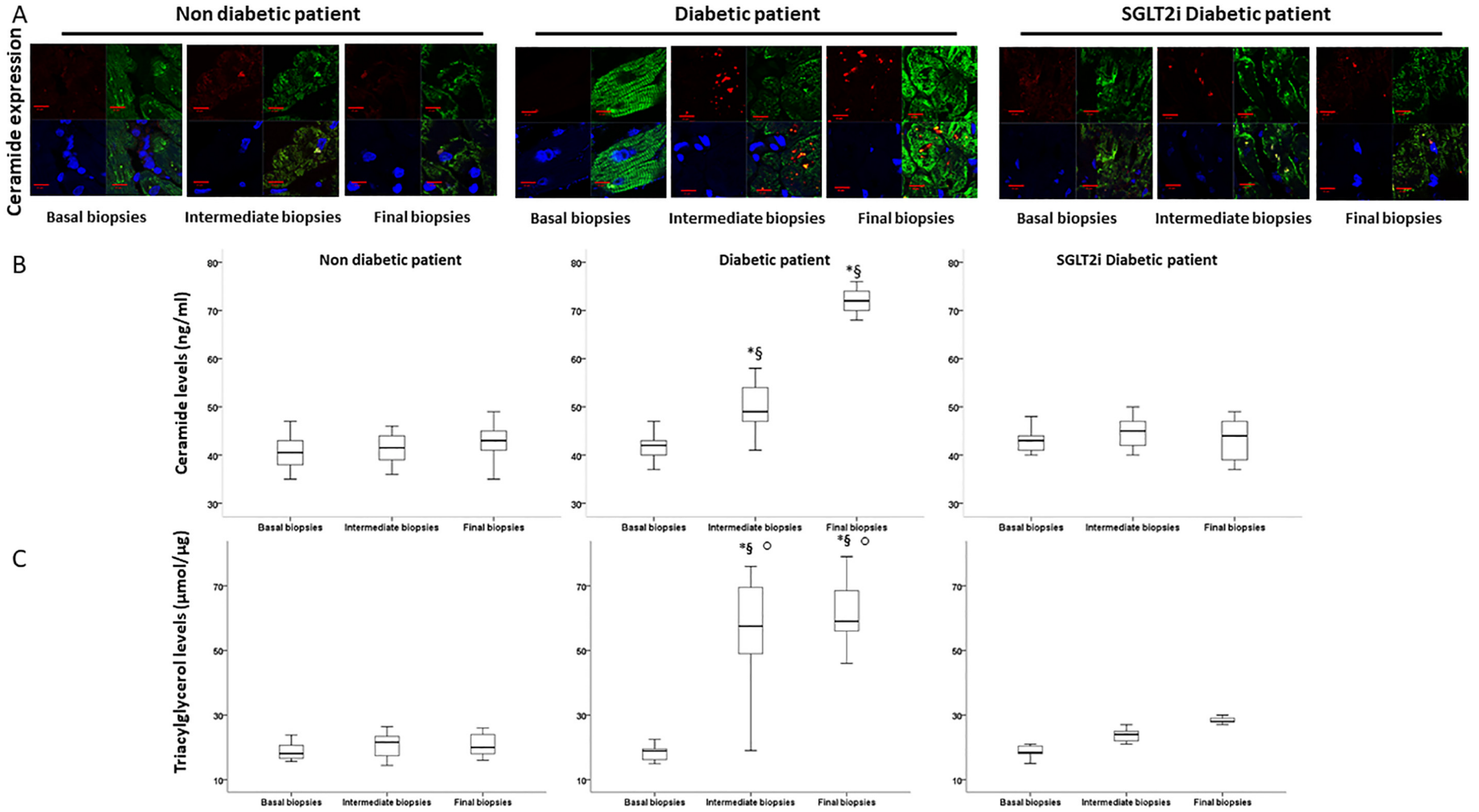

Fig. 7. Ceramide and triacylglycerol in myocardial biopsies at basal, intermediate, and final evaluations. Panel A, Confocal laser-scanning microscope images showing the ceramide content (red) in deparaffinized explanted heart sections from patients without diabetes, non-SGLT2i-treated patients with diabetes, and SGLT2i-treated patients with diabetes at 1–4 weeks (Basal), 5–12 weeks (Intermediate), and up to 48 weeks (Final, end of 12-month follow-up) after HTX. Cardiac troponin T (green) was used to localize the immunofluorescence signal in cardiomyocytes, while 4′,6-diamidino-2-phenylindole (DAPI; 5 μg/ml) staining was used for nuclei counterstaining (blue). Upper left, ceramide; upper right, troponin T; lower left, DAPI; lower right, merged. Scale bar = 10 μm. Panel B, Ceramide myocardial content in heart specimens from biopsies of patients without diabetes, non-SGLT2i-treated patients with diabetes, and SGLT2i-treated patients with diabetes at 1–4 weeks (Basal), 5–12 weeks (Intermediate), and up to 48 weeks (Final, end of 12-month follow-up) after HTX. Panel C, Triacylglycerol myocardial content in heart specimens from biopsies of patients without diabetes, non-SGLT2i-treated patients with diabetes, and SGLT2i-treated patients with diabetes at 1–4 weeks (Basal), 5–12 weeks (Intermediate), and up to 48 weeks (Final, end of 12-month follow-up) after HTX. Boxplot showing the median, 25th and 75th percentiles, and range. *$P < 0.05$ vs. patients without diabetes, §$P < 0.05$ vs. SGLT2i-treated patients with diabetes, °$P < 0.05$ vs. basal values.

follow-up period, both triacylglycerol and ceramide levels were higher in specimens from non-SGLT2i-treated patients with diabetes than in those without diabetes or those treated with SGLT2i ($P < 0.01$) (Fig. 7). Remarkably, at the final follow-up, triacylglycerol and ceramide levels were significantly higher in samples from non-SGLT2i-treated patients with diabetes than in specimens from patients without diabetes and SGLT2i-treated patients with diabetes (Fig. 7). Scatter graphs show that the myocyte ceramide and triacylglycerol level changed varied with the JunD level (Fig. 8).

As shown by the scatter graphs, heart function (ejection fraction, E/e′ ratio, and TAPSE), JunD, insulin receptors, and myocardial lipid level (ceramide and triacylglycerol levels) can be divided into distinct groups based on three "clouds of data." Finally, the analysis with the mixed model (Supplementary Table 1) identified a significant difference between groups and between times, and a between group and time interaction. Moreover, post-hoc analysis showed significant differences compared to patients without diabetes. Finally, no sex-related differences were observed in JunD, IRS1, IRS2, PPARϒ, ceramide, or triacylglycerol myocardial levels (Supplementary Fig. 3).

4. Discussion

We show for the first time the association between the JunD/PPAR-γ pathway and early lipotoxic diabetic heart dysfunction in humans, which was partially prevented by the concomitant use of SGLT2i (Graphical abstract). The specific pathogenic contribution of JunD expression correlated with PPAR-γ and lipid accumulation (ceramide and triacylglycerol) measured in heart specimens in this model.

We investigated the early detrimental effects of diabetes on the myocardial JunD/PPAR-γ pathway, which is involved in human diabetic cardiomyopathy progression, such as in healthy hearts transplanted into recipients with diabetes. Here, we observed that the JunD/PPAR-γ pathway in cardiomyocytes might contribute to the initiation and progression of heart dysfunction through lipotoxicity, as evidenced by a progressive increase of ceramide in cardiomyocytes from healthy hearts implanted in patients with diabetes. Cardiomyocyte JunD/PPAR-γ pathway disorder may be a pivotal pathogenic event related to insulin resistance, as shown by scatter graphs showing that cardiomyocyte insulin substrates varied when JunD expression increased. Although we cannot evaluate these data using a regression because, as seen in the graphs, we have three different groups of data, the analysis with a mixed model identified a significant difference between groups, between times, and a between groups and times interaction. Moreover, post-hoc analysis showed significant differences from the results in patients without diabetes. Thus, we hypothesized that progressive cardiomyocyte lipid accumulation, linked to JunD/PPAR-γ pathway overexpression, may interfere with heart function, as indicated by the correlation between JunD expression and both diastolic and systolic impairments. Moreover, we observed that JunD/PPAR-γ pathway derangement begins early in transplanted healthy hearts of patients with diabetes but not in patients without diabetes, as demonstrated by the increase in the cardiomyocyte JunD/PPAR-γ pathway activity 3 months after heart transplantation but not in the first EMB after heart transplantation. Therefore, the diabetic milieu can promptly alter the JunD/PPAR-γ pathway and lipid metabolism in cardiomyocytes. Indeed, the myocyte ceramide and triacylglycerol levels changed with the JunD levels. Finally, we showed that increased expression of JunD was associated with cardiac dysfunction, independent of body mass index (BMI), heart rate, and blood pressure, in patients with diabetes 12 months after HTX.

As a background for these associations, we observed that myocardial insulin resistance was higher in healthy transplanted hearts in recipients with diabetes than in recipients without diabetes. These phenomena were more evident during follow-up progression, stressing the early tandem action of diabetic milieu and metabolic disease in the pathogenesis of diabetic cardiomyopathy. Because systemic insulin resistance correlated with JunD expression, we hypothesized that the metabolic milieu of patients with diabetes has a detrimental role in the early progression of diabetic cardiomyopathy.

Strikingly, the present study suggested an inhibitory effect of SGLT2i on the JunD/PPAR-γ pathway in HTX recipients with diabetes. Indeed, with equal risk factors, SGLT2i-treated patients with diabetes showed a slower increase in myocardial JunD/PPAR-γ pathway activity, myocardial insulin resistance, lipid accumulation, and heart dysfunction. Thus, the concomitant use of SGLT2i potently reversed the detrimental effects caused by the diabetic milieu. Previous data showed that SGLT2i reduced death from cardiovascular causes and improved heart function in type 2 diabetes mellitus through anti-hyperglycemic effects and non-glycemic effects, such as reducing visceral and ectopic fat [19]. To the best of our knowledge, this is the first study to show a reduction in JunD, PPAR-γ, and ceramide levels in the human diabetic heart following SGLT2i treatment.

SGLT2i may act on systemic and cardiac insulin resistance, as evidenced by the observation that both HOMA-IR and cardiomyocyte insulin receptor levels were improved by SGLT2i therapy. SGLT2i influence cardiac energy metabolism, breaking the vicious circle between HF and IR and mediating cardioprotective effects by regulating

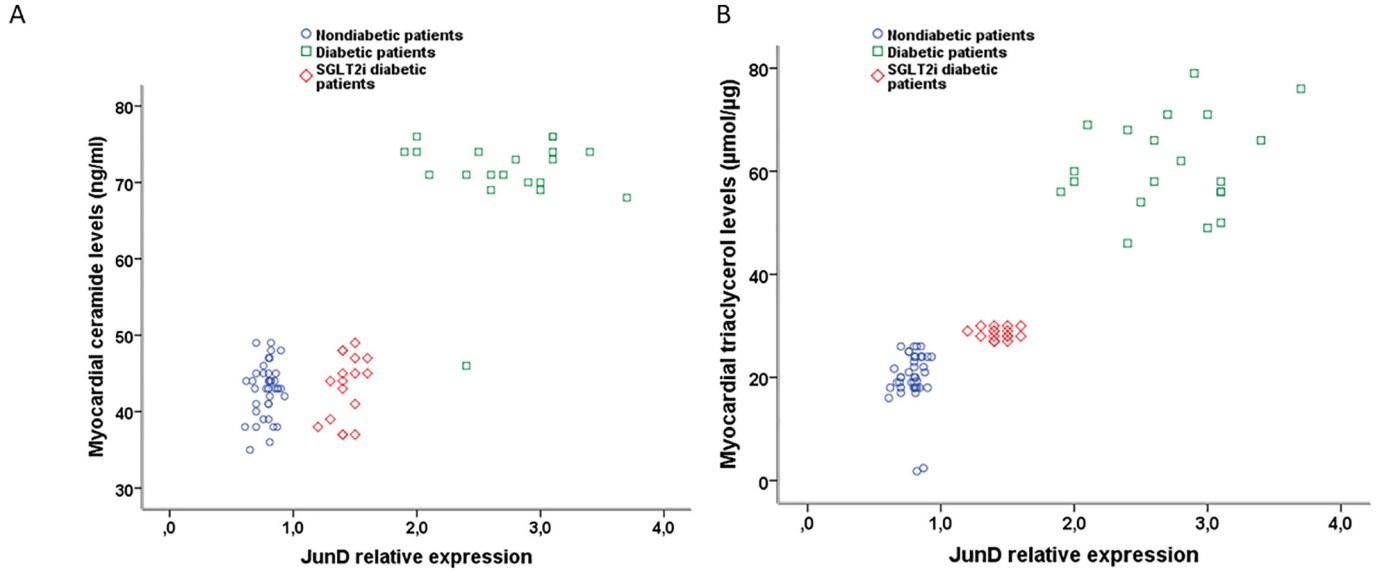

Fig. 8. Scatter graphs. Panel A, Scatter graph of JunD and myocardial ceramide levels. Panel B, Scatter graph of myocyte JunD expression and myocardial triacylglycerol level.

mitochondrial function, modulating glucose metabolism, enhancing fatty acid metabolism, and shifting to ketone body metabolism [20,21]. Therefore, SGLT2i can increase glucose and fatty acid utilization and shift the myocardial fuel from glucose to ketone bodies and free fatty acids. This transformation can increase the energy production of the diabetic heart, along with improvements of heart remodeling, demonstrating the therapeutic potential of SGLT2i in heart failure and insulin resistance [22]. In addition, multiple large-scale clinical studies have confirmed the beneficial effects of SGLT2i on cardiovascular events and explored the clinical benefits of SGLT2 in regulating metabolism [23,24]. However, most clinical trials are limited to patients with clinically evident heart failure. In our study, we show for the first time the role of SGLT2i in preventing metabolic derangements from leading to heart dysfunction. Thus, JunD/PPAR-γ pathway regulation might be associated with better cardiac function in patients with type 2 diabetes treated with SGLT2i than in patients with diabetes not receiving such treatment. This unique model showed that patients with type 2 diabetes treated with SGLT2i maintained normal cardiac function after 12 months of follow-up.

4.1. Study limitations

First, this study's major limitation is its observational nature and the inability to determine a causal relationship with molecular data. However, the study population is very powerful, and the observations will likely stimulate additional mechanistic studies. Second, our study is not a multicenter study, and thus we need to extend our observations to a larger cohort of patients. Third, immunosuppressive therapy could affect the JunD/PPAR-γ pathway. However, we observed that the progressive increase in the JunD/PPAR-γ pathway was blunted by SGLT2i therapy during immunosuppression. Fourth, HOMA-IR as an index of systemic insulin resistance may have some limitations [25,26]. The limitations of HOMA-IR should be considered in individuals with very low BMI, high fasting glucose levels, and mixed-race populations. Due to the strict selection criteria for HTX, our study population had similar BMI, fasting glucose levels, and only included Caucasian patients. Moreover, we evaluated the phosphorylation of IRS1 and PPAR-γ. Therefore, we hypothesize that IRS1 and PPAR-γ activities are modulated by diabetes and SGLT2i therapy. Finally, it is impossible to discern any differences between individual SGLT2i due to the low number of cases where they were used. Despite these limitations, we provide first evidence of early (within 12 months) impairments of metabolic mechanisms implicated in the pathogenesis of human diabetic cardiomyopathy. Thus, the major goal of our study was to provide a new real-life study to investigate the early effects of the diabetic milieu on the heart. Moreover, JunD could be a new target for the early prevention of diabetic cardiomyopathy and subsequent heart failure.

5. Conclusion

Our human study revealed a new molecular mechanism by which SGLT2i may act directly on the myocardium to prevent diabetic heart dysfunction. These findings improve our understanding of the pathophysiology of diabetic cardiomyopathy and may provide a novel stage for SGLT2i therapy to prevent heart dysfunction in patients with type 2 diabetes.

Funding

Progetti di Rilevante Interesse Nazionale (PRIN), N: 2017FM74HK_002, Research Italy.

Availability of data and materials

The datasets used and analyzed during the current study are available from the corresponding author upon reasonable request.

Clinical trial registry

clinicaltrialgov.com NCT03546062.

Vanvitelli University Ethical Committee number

438 for study on diabetic cardiomyopathy.

CRediT authorship contribution statement

Design: Raffaele Marfella, Giuseppe Paolisso
Conduct/data collection: Celestino Sardu, Cristiano Amarelli, Marisa De Feo, Ciro Maiello
Analysis: Nunzia D'Onofrio, Lucia Scisciola, Maria Luisa Balestrieri, Claudio Napoli, Maria Consiglia Trotta, Vincenzo Grimaldi, Gelsomina Mansueto, Salvatore Esposito, Michele D'Amico, Paolo Golino, Giuseppe Signoriello
Writing manuscript: Raffaele Marfella, Giuseppe Paolisso.

Declaration of competing interest

The authors declare that they have no conflict of interest.

Acknowledgments

The authors are grateful to Dr. Luigi Ruggiero (Geriatric Unit of Università degli Studi della Campania "Luigi Vanvitelli") for important work in the clinical evaluation of patients admitted to our department.

Appendix A. Supplementary data

Supplementary data to this article can be found online at https://doi.org/10.1016/j.metabol.2021.154936.

References

[1] Jia G, Hill MA, Sowers JR. Diabetic cardiomyopathy: an update of mechanisms contributing to this clinical entity. Circ Res. 2018;122:624–38.
[2] Yancy CW, Jessup M, Bozkurt B, Butler J, Casey Jr DE, Colvin MM, et al. 2017 ACC/AHA/HFSA focused update of the 2013 ACCF/AHA guideline for the management of heart failure: a report of the American College of Cardiology/American Heart Association Task Force on Clinical Practice Guidelines and the Heart Failure Society of America. J Am Coll Cardiol. 2017;70:776–803.
[3] Iribarren C, Karter AJ, Go AS, Ferrara A, Liu JY, Sidney S, et al. Glycemic control and heart failure among adult patients with diabetes. Circulation. 2001;103:2668–73.
[4] Marwick TH, Ritchie R, Shaw JE, Kaye D. Implications of underlying mechanisms for the recognition and management of diabetic cardiomyopathy. J Am Coll Cardiol. 2018;71:339–51.
[5] Kovacic JC, Castellano JM, Farkouh ME, Fuster V. The relationships between cardiovascular disease and diabetes: focus on pathogenesis. Endocrinol Metab Clin North Am. 2014;43:41–57.
[6] Costantino S, Akhmedov A, Melina G, Mohammed SA, Othman A, Ambrosini S, et al. Obesity-induced activation of JunD promotes myocardial lipid accumulation and metabolic cardiomyopathy. Eur Heart J. 2019;40:997–1008.
[7] Hussain S, Khan AW, Akhmedov A, Suades R, Costantino S, Paneni F, et al. Hyperglycemia induces myocardial dysfunction via epigenetic regulation of JunD. Circ Res. 2020;127:1261–73.
[8] Panchapakesan U, Pegg K, Gross S, Komala MG, Mudaliar H, Forbes J, et al. Effects of SGLT2 inhibition in human kidney proximal tubular cells—renoprotection in diabetic nephropathy? PLoS One. 2013;8(2):e54442.
[9] Varzideh F, Kansakar U, Santulli G. SGLT2 inhibitors in cardiovascular medicine. Eur Heart J Cardiovasc Pharmacother. 2021;7(4):e67–8.
[10] Yang Y, Zhao C, Ye Y, Yu M, Qu X. Prospect of sodium-glucose co-transporter 2 inhibitors combined with insulin for the treatment of type 2 diabetes. Front Endocrinol (Lausanne). 2020;11:190.
[11] Zhang A, Luo X, Meng H, Kang J, Qin G, Chen Y, et al. Sodium-glucose co-transporter 2 inhibitors reduce the risk of heart failure hospitalization in patients with type 2 diabetes mellitus: a systematic review and meta-analysis of randomized controlled trials. Front Endocrinol (Lausanne). 2021;11:604250.
[12] Tanaka A, Node K. How should we monitor the cardiovascular benefit of sodium-glucose cotransporter 2 inhibition? Cardiovasc Diabetol. 2020;19:206.
[13] Marfella R, Amarelli C, Cacciatore F, Balestrieri ML, Mansueto G, D'Onofrio N, et al. Lipid accumulation in hearts transplanted from nondiabetic donors to diabetic recipients. J Am Coll Cardiol. 2020;75:1249–62.

[14] Galiè N, Humbert M, Vachiery JL, ESC Scientific Document Group. ESC/ERS guidelines for the diagnosis and treatment of pulmonary hypertension: the Joint Task Force for the Diagnosis and Treatment of Pulmonary Hypertension of the European Society of Cardiology (ESC) and the European Respiratory Society (ERS): endorsed by: Association for European Paediatric and Congenital Cardiology (AEPC), International Society for Heart and Lung Transplantation (ISHLT). Eur Heart J. 2015;2016(37):67–119.

[15] Badano LP, Miglioranza MH, Edvardsen T, Colafranceschi AS, Muraru D, Bacal F, et al. Document reviewers. European Association of Cardiovascular Imaging/Cardiovascular Imaging Department of the Brazilian Society of Cardiology recommendations for the use of cardiac imaging to assess and follow patients after heart transplantation. Eur Heart J Cardiovasc Imaging. 2015;16:919–48.

[16] Galderisi M, Cosyns B, Edvardsen T, Cardim N, Delgado V, Di Salvo G, et al. 2016–2018 EACVI Scientific Documents Committee. Standardization of adult transthoracic echocardiography reporting in agreement with recent chamber quantification, diastolic function, and heart valve disease recommendations: an expert consensus document of the European Association of Cardiovascular Imaging. Eur Heart J Cardiovasc Imaging. 2017;18:1301–10.

[17] Balestrieri ML, Servillo L, Esposito A, D'Onofrio N, Giovane A, Casale R, et al. Poor glycaemic control in type 2 diabetes patients reduces endothelial progenitor cell number by influencing SIRT1 signalling via platelet-activating factor receptor activation. Diabetologia. 2013;56:162–72.

[18] D'Onofrio N, Servillo L, Giovane A, Casale R, Vitiello M, Marfella R, et al. Ergothioneine oxidation in the protection against high-glucose induced endothelial senescence: involvement of SIRT1 and SIRT6. Free Radic Biol Med. 2016;96:211–22.

[19] Komiya C, Tsuchiya K, Shiba K, Miyachi Y, Furuke S, Shimazu N, et al. Ipragliflozin improves hepatic steatosis in obese mice and liver dysfunction in type 2 diabetic patients irrespective of body weight reduction. PLoS One. 2016;11(3):e0151511.

[20] Kang A, Jardine MJ. SGLT2 inhibitors may offer benefit beyond diabetes. Nat Rev Nephrol. 2021;17:83–4.

[21] Gronda E, Jessup M, Iacoviello M, Palazzuoli A, Napoli C. Neurohormonal activation and heart failure development. J Am Heart Assoc. 2020;9:e018889. https://doi.org/10.1161/JAHA.120.018889.

[22] Wang X, Ni J, Guo R, Li L, Su J, He F, et al. SGLT2 inhibitors break the vicious circle between heart failure and insulin resistance: targeting energy metabolism. Heart Fail Rev. Mar 12 2021. https://doi.org/10.1007/s10741-021-10096-8.

[23] Verma S, Rawat S, Ho KL, Wagg CS, Zhang L, Teoh H, et al. Empagliflozin increases cardiac energy production in diabetes: novel translational insights into the heart failure benefits of SGLT2 inhibitors. JACC Basic Transl Sci. 2018;3:575–87.

[24] Das SR, Everett BM, Birtcher KK, Brown JM, Januzzi Jr JL, Kalyani RR, et al. 2020 expert consensus decision pathway on novel therapies for cardiovascular risk reduction in patients with type 2 diabetes: a report of the American College of Cardiology Solution Set Oversight Committee. J Am Coll Cardiol. 2020;76:1117–45.

[25] Kang ES, Yun YS, Park SW. Limitation of the validity of the homeostasis model assessment as an index of insulin resistance in Korea. Metabolism. Feb 2005;54(2):206–11.

[26] Pisprasert V, Ingram KH, Lopez-Davila MF, Munoz AJ, Garvey WT. Limitations in the use of indices using glucose and insulin levels to predict insulin sensitivity: impact of race and gender and superiority of the indices derived from oral glucose tolerance test in African Americans. Diabetes Care. 2013;36:845–53.